Material Characterization of GFRP Bars in Compression using a New Test Method

Koosha Khorramian[1] and Pedram Sadeghian[2]

ABSTRACT: This paper presents a new test method for determining the mechanical properties of glass fiber-reinforced polymer (GFRP) composite bars in compression, namely the compressive strength, compressive modulus of elasticity, ultimate crushing strain, and compressive stress-strain curves of the bars. The contribution of GFRP bars in compression is currently neglected by major design guidelines related to GFRP-reinforced concrete columns. However, the demand for using GFRP bars is increasing since multiple researchers have shown the effectiveness of the bars in concrete columns. Thus, the need for characterization of the mechanical properties of GFRP bars is increasing, while there is no standardized test method to evaluate the compressive properties of these bars. Therefore, in this paper, a new test method is proposed for evaluating the compressive characteristics of GFRP bars. The proposed test method was examined through testing a total of 35 specimens. It was observed that the test method was able to evaluate the compressive characteristics of the GFRP bars successfully. Three different modes of compressive failure were observed which were related to the crushing of GFRP bars in different locations in the bar, but no premature failure or bar buckling was observed. Moreover, a comparison between tensile and compression characteristics of the GFRP bars showed that the tensile test results is not sufficient to estimate the compressive characteristics and performing compression test is necessary.

https://doi.org/10.1520/JTE20180873

[1] Department of Civil and Resource Engineering, Dalhousie University, 1360 Barrington street, Halifax, NS, B3H 4R2 Canada, email: Koosha.Khorramian@dal.ca

[2] Department of Civil and Resource Engineering, Dalhousie University, 1360 Barrington street, Halifax, NS, B3H 4R2 Canada (Corresponding author), email: Pedram.Sadeghian@dal.ca

KEYWORDS: Test Method, GFRP Bar, Compression, Crushing, Material Characterization

INTRODUCTION

The determination of compressive characteristics of glass fiber-reinforced polymer (GFRP) composite bars including the compressive strength, modulus of elasticity, and crushing strain, as well as obtaining stress-strain relationship is the subject of the current paper. The knowledge of these characteristics assists the analysis and design of structural concrete members reinforced with GFRP bars which are under compression. These members could be concrete columns, flexural members (i.e. bridge decks, slabs, and beams), and reinforced walls (i.e. concrete or masonry walls) in which GFRP bars were subjected to compressive stresses. In addition, the deflection of the concrete members with GFRP bars in compression is influenced by the compressive modulus of elasticity of GFRP bars. Despite of numerous researches on concrete members reinforced with GFRP bars, there is no standardized test method to determine the compressive characteristics of GFRP bars.

Due to the lack of such a test method, there are some doubts and gaps in terms of the behavior of GFRP bars in compression which led to lack of information on their compressive characteristics. For example, the current American guideline for the design of fiber-reinforced polymer (FRP) bars in concrete structures [1] neglects the contribution of GFRP bars in compression and allows the designer to replace them with the concrete for the design procedure. Moreover, the Canadian guideline for design and construction of building structures with FRP [2] allows the use of GFRP bars in concentrically loaded columns if their contribution in the strength of the column is neglected. Despite of the limitations, recent studies have shown that neglecting the contribution of compressive GFRP bars in concrete columns is conservative [3, 4, 5, 6, 7, 8]. Recent studies have already changed the trend of the very recent design guidelines. For example,

in the draft of the Canadian highway bridge design code [9] which has been revised to be published in 2019, the longitudinal FRPs are allowed for members subjected to combined axial and flexural loads up to a strain level of 0.002 mm/mm. Therefore, the new trend is toward the acceptance of GFRP bars in compression that emphasizes the necessity of having a standardized test method for evaluating the compressive characteristics of GFRP bars.

It should be noted that recently there have been researches on the seismic behavior of the GFRP reinforced concrete columns [10, 11]. The results of their studies indicated that GFRP bars can be used as internal reinforcement in ductile columns. Therefore, compressive characteristics of the columns are required for design purposes. In addition, in terms of seismic applications, unlike the conventional design in which the neglection of GFRP bars in compression is conservative, the neglection of the compressive bars might cause lower expectations in the ultimate load levels and unconservative seismic designs. For concrete columns reinforced with FRP bars whose modulus of elasticity are different than concrete modulus of elasticity, the stiffness of columns and, in turn, their contribution in resisting the lateral load would be different. Therefore, neglecting FRP bars may relate the share of each column from the lateral loads only to the column size instead of real stiffness of the columns. Thus, a knowledge of compressive characteristics is crucial which is not addressed in any standardized guideline.

There have been multiple studies on the characterization of GFRP bars in compression. Kobayashi and Fujisaki [12] studied the compressive behavior of GFRP bars by conducting an experimental program in which the specimens were built so that GFRP bars were embedded in concrete prisms. The specimens were built to have a small space at the center (5 mm) and they were anchored to the testing machine using carbon fiber cones. It was mentioned that the concrete prisms were fixed in the testing machine and the load applied only to the FRP bar at the center

[12]. The compressive strength of GFRP bars were reported as 30% of their tensile capacity. However, it should be mentioned that the small space between two concrete prisms was 5 mm which in comparison to the tested bar diameters (varies from 6 to 10 mm), gives a ratio of free length to diameter of 0.5 to 0.83. This small ratio might cause stress concentration in the specimen plus increasing the chance of the specimen not to experience the unidirectional state of stress which leads to lower ultimate loads.

Dietz et al. [13] published a technical note on the properties of 45 GFRP bars with different slenderness ratios which were tested in compression. All the tested bars were provided by the same manufacturer. In their study, a single bar size of #15 (15 mm diameter) was tested using a length variation between 50 to 380 mm. In the study, there was an observation of three different modes of failure including crushing, buckling, and combined buckling and crushing. Two threaded rods were used in the test set-up to hold the specimens and tie them to the testing machine. The bars were inserted inside the threaded rods from their bottom and top, using a hole with a diameter of 17.5 mm which was slightly wider than the bar diameter and allows slight rotation at the ends of the bars. Similar modulus of elasticity in tension and compression was reported [13]. However, the observations showed 50% less strength in compression in comparison to in tension for the tested GFRP bars. The free length to diameter ratios of the tested GFRP bars varied between 3.33 to 25.33, and it was concluded that the GFRP bars tested with free length to diameter ratio of less than 7.33 can be considered as nonslender. Moreover, it was concluded that the modulus of elasticity of the bars in compression and tension are approximately equal while the compressive strength of FRP bars is about 50% of their tensile strength.

Khan et al. [14] tested five GFRP and five carbon FRP (CFRP) bars. The GFRP bars were 80 mm long with a diameter of 15.9 mm, and were tested by adopting ASTM D695 [15] which is

the standard method for compressive properties of rigid plastics. Their tests included the use of two parallel steel plates at the ends of the GFRP bars and using a displacement control approach with a rate of 1.0 to 1.3 mm/min. The specimens were directly located between the steel plates to simplify ASTM D695 [15] by replacing the hardened end blocks with flat and high strength steel plates. It was reported that the failure happened due to separation of fibers which might be a result of failure of the resin [14]. It was observed that the modulus of elasticity and strength of GFRP bars in tension were 65% and 35% higher than their compressive counterparts, respectively.

Tavassoli et al. [11] studied circular concrete columns reinforced with GFRP bars under simulated seismic loading. A part of the study was dedicated to testing 15 GFRP bars from two different manufacturers. Their tests were focused on GFRP bars with a diameter of 25 mm with various free lengths that were chosen based on the spiral pitch in the studied concrete columns. The spiral pitch varied between 50 to 275 mm which gives the ratio of free length to diameter of 2 to 11 [11]. It should be noted that steel rods with a hole that holds the GFRP bars in the machine was used for testing which was similar to Dietz proposed method [13]. It was observed that the compressive strength of GFRP bars were about 50% of their tensile strength while their modulus of elasticity in compression and tension were similar.

Overall, there were various test fixtures for the characterization of GFRP bars in compression by researchers [12, 13, 14, 11]. However, there were different observations on the compressive strength and modulus of elasticity of these proposed test methods as mentioned earlier. The free length to diameter ratio was varied from test to test, and the modes of failure were either buckling of the bar, buckling of the fibers after separation of the resin, or end crushing. The latter might cause observations which showed less compressive strength for GFRP bars due to buckling (for high free length to diameter ratios) or because of biaxial state of stress (for very small

free length to diameter ratios). In addition, for some of the proposed test methods, there was a room for end rotation that enabled the GFRP compressive coupon to experience a combined flexural and axial loading which, in turn, resulted in lower compressive capacity. The other issue would be crushing at the end of GFRP bars whose effect on the strength should be studied. Furthermore, it should be highlighted that in addition to test methods, the quality of FRP bar manufacturing and evolution of FRP bars might be an effective parameter in diversity of the reported values for strength and modulus of elasticity of bars at different dates. For example, recent reports of strength and modulus of elasticity of GFRP bars showed higher values than the values in the earlier studies. A summary of test methods used by previous researchers is presented in Table 1.

There is a clear gap in terms of capturing the material failure of GFRP bars or at least giving a better prediction of the crushing strength of GFRP bars which is distinct from their buckling. Therefore, the authors' research group started to design a new test method by considering the criteria for GFRP coupons to experience a uniform unidirectional state of stress, to avoid the buckling of GFRP bars or fibers due to separation of resin, and to avoid combined flexural and axial loading of GFRP compressive coupons. The idea of designing a steel cap filled with bonding agent and limiting the free length to diameter ratio of bars were motivations of the current paper. The authors' research group attempted testing GFRP bars in compression [5, 4] and later presented a preliminary report [16] on the test method. The current paper expands the research to a detailed test method and a comprehensive research program with a total of 35 test specimens with three different bar types from three different manufacturers. Moreover, more in depth discussion and investigation of failure modes and their correlation to the compressive characteristics is discussed.

RESEARCH SIGNIFICANCE

Available test data and research on the compressive behavior of GFRP bars is very limited due to lack of a standardized and reliable test method and the neglection of their contribution in structural members when used in compression. However, the current trend of the engineering communities is toward the acceptance of their usage in compression in structural members because of recent studies on the behavior of GFRP-reinforced concrete columns. On the other hands, various modulus of elasticities and strengths have been reported for GFRP bars in compression by researchers using different methods. However, different modes of failures such as buckling of GFRP bars, separation of resin and buckling of fibers, end crushing of GFRP bars, and different testing conditions which may cause undesired eccentricity results in an underestimation of the compressive strength of GFRP bars in material level. Therefore, this study proposes a test method to characterize the compressive behavior of GFRP bars and presents an experimental study to examine the proposed test method that addresses the issues.

PROPOSED TEST METHOD

In this section, a new method is proposed for testing GFRP bars in compression. The proposed test method determines the mechanical properties of GFRP bars including the compressive strength, compressive modulus of elasticity, ultimate compressive strain, and stress-strain curve in compression. As shown in Fig. 1, the test coupon consists of a GFRP bar which is positioned in a mechanical testing machine and loaded with a displacement rate of 0.5 mm/min up to the failure while the values of axial load, strain, and displacement are recording. The compressive coupon consists of two steel plates, two steel rings, two anchoring adhesive agents, and a GFRP bar, as shown in Fig. 1. The steel plates are square with a width of four times the diameter of the GFRP

bar and a thickness of at least 5 mm. The steel rings are proposed to have a depth of equal to the diameter of the bar, a diameter twice as wide as the diameter of GFRP bar and a minimum thickness of 3.3 mm (this thickness was the minimum thickness of plate with which the tests were performed successfully, and it was chosen based on availability in the lab). The steel rings are welded to the center of the steel plates on top and bottom of the GFRP bar to form a solid unit, called steel cap in this text. The functions of steel cap are holding the GFRP bar, alignment, gripping action, and strengthening the ends of the specimens. It should be mentioned that the ease of alignment and gripping are the advantages of using the steel cap filled with a high strength, fast setting anchoring adhesive. To align GFRP bar and steel cap, the alignment is controlled once GFRP inserts in the steel cap filled with adhesives. The ends of the GFRP bars must be cut perpendicular to the longitudinal axis of bars, and the bars must be positioned at the center of the steel caps. Then, a level at the flat surface of GFRP bar can give the required alignment. Using a laser alignment tool can ensure the GFRP bar is centered and perpendicular to the steel cap. Once the adhesive is set, the procedure should be repeated for the second steel cap. The coupons can be prepared as quickly as 20 minutes for both sides using a fast setting adhesive (without considering the time for strain gauging and building steel caps). After the adhesive was set, the steel caps provided a solid capping for the GFRP bar to prevent any premature crushing at the ends. The lateral confinement provided for the end of the GFRP bar by the steel rings filled with adhesive assist avoiding localized crushing of the GFRP bar at the ends. It is important to prepare the coupon accurately to avoid any accidental eccentricity and to give a uniform unidirectional compressive stress in the testing length of the GFRP bar.

The overall length of the GFRP bar is proposed to be four times its nominal, which gives a free length to diameter ratio of 2, as shown in Fig. 1. It should be noted that the free length of

GFRP bars tested in tension shall be 40 times greater than their diameter according to the standard method for testing FRP bars in tension, ASTM D7205 [17]. However, in tension there is no concern about the buckling of GFRP bars or secondary bending moments due to additional displacement at the middle of the bar. Therefore, the standards for compressive testing of materials define limitations on the free length to diameter or width ratio to avoid buckling and reach the material failure. For instance, the standard test method for testing polymer matrix composites using combined loading compression test fixture, ASTM D6641 [18], suggests the prepration of compressive coupons with tabs for flat FRP laminates which gives a free length between tabs that is as short as the width of the specimen. Moreover, the standard test method for testing concrete cylinders in compression, ASTM C39 [19], recommends the free length over diameter ratio of 2.

TEST METHOD IMPLEMENTATION

In this section, an experimental program consisting of testing of 35 compressive coupons built according to the proposed test method is explained. The section includes test matrix, fabrication process, test set up, and instrumentation.

Test Matrix

Table 2 presents the test matrix for the compressive GFRP coupons which were categorized in seven groups. Each group consists of five identical test specimens which were identified by an ID code as “Gx-y”, where “G” stands for group, “x” represents the group number and “y” shows the specimen number in each group. The GFRP bars used in different groups were different from the other groups in terms of bar size, manufacturer, and the tensile characteristics. Overall, 35 GFRP coupons were tested from three different manufacturers, with three different bar sizes, and seven different tensile characteristics. The manufacturers were ASLAN 100 (Seward, NE, USA), V-

ROD (Toronto, ON, Canada), TUFBAR (Edmonton, AB, Canada) that are named as “A”, “B”, and “C”, respectively, as presented in Table 2. All bars were made of glass fibers and vinyl ester resin. The fiber weight fraction of bars was at least 70%, 83%, and 80% which were reported by manufacturer A, B, and C, respectively. The tensile strength and modulus of elasticity of GFRP bars that is presented in Table 2 were reported by the manufacturers. In addition, the first three groups of specimens were adopted from the previous studies by the same research group as addressed in Table 2. However, all the specimens were built using the proposed test method in this paper.

Specimen Fabrication

The preparation of the specimens directly relates to the quality of the test results, since the alignment and capping requirements must be satisfied in the preparation phase. Fig. 2 presents the process of the of the preparation of the compressive GFRP coupon. The steel cap, which consists of a steel plate welded to a steel ring, was located at a horizontal and flat surface. Afterwards, the steel cap was filled with a quick set anchoring adhesive. Then, the GFRP bar, whose end surface was flat and perpendicular to the longitudinal axis (a jig was used to ensure proper cutting), was positioned at the middle of the steel cap and inserted into the adhesive until it touched the steel plate. The excessive adhesive was removed until the surface of the adhesive was flushed with the edge of steel ring. At this stage, a level was placed at the top surface of the bar to make sure that the bar was not inclined. The location of the center of the capping was marked and the GFRP bar inserted at the center of the capping. After the adhesive was set, the same procedure repeated for the other end of the bar to have both steel caps installed properly at the ends of the GFRP bar.

After the installation of the steel caps, the surface of the GFRP bar at the mid-height were machined shallowly. In other words, the surface was flatten using a milling machine and file for

the installation of the strain gauges at two opposite sides of the bar (which gives about 1 to 2 mm depth of the machined area). Afterwards, a high strength glue was applied on the machined surface. Once the glue was set, a file was used to flatten the surface, and two different sand papers (one course and one fine sand papers) were used to polish the surface. Fig. 3 shows the prepared GFRP coupons prepared according to the proposed test method in this study. To attain consistent and reliable results, the application of strain gauges directly on the machined surface is not suggested due to observation of unusual strain gauge records for specimens tested without proper surface preparation.

Test Setup and Instrumentation

The schematic test set-up is presented in Fig. 4, where the GFRP coupon is located in a mechanical testing machine. The test specimen must be located properly at the center of the testing machine to be aligned with the machine to produce pure compression loading. Moreover, to avoid accidental eccentricities, a spherical platen was placed beneath the compressive coupon which enables small rotations and the self-centering action. Furthermore, two thick steel plates were placed at the top and the bottom of the specimen (25 mm-thick plates were used in this study), as shown in Fig. 4, to provide smooth surface at the ends of the specimen and to allow a uniform state of the stress. It should be emphasized that the weight of these plates was neglected since their corresponding load was very small in comparison to the applied load (i.e. almost 0.02% of the ultimate load). Fig. 5 shows one of the specimens in the testing machine. To record the data, there were two strain gauges model FLA-6-350-11 (Tokyo Sokki Kenkyujo Co., Ltd., Japan) with the length of 11 mm, a gauge length of 6 mm, and a gauge resistance of 350 Ω. The size of strain gauge was selected based on availability to the research group. However, as the free length of the bar is proposed to be twice the diameter of the bar, using strain gauge with a gauge length of more

than diameter of the bar is not recommended to be located within the region of the bar with uniform stress state. The strain gauges were longitudinally installed at the opposite sides and at the middle of the GFRP bar, whose average was considered as the strain value used for the calculation of modulus of elasticity. Installation of two strain gauges and reporting the results as the average value was suggested by ASTM D7205 [17] for testing FRP bars in tension, which was adopted in this study for testing GFRP bars in compression. The specimens were tested by a 2 MN self-reaction Instron machine (Model 5596) with a displacement control approach using a testing rate of 0.5 mm/min. The tests were finished in about 5 minute which was compatible with the suggested rates for the tensile test of FRP bars [17]. The sampling rate was 10 data per second which recorded the data including axial strain, axial load, and axial stroke displacement from the machine.

TEST RESULTS AND DISCUSSION

The results and findings from the experimental tests are presented in the following which includes a discussion on the observation of the modes of failure, the stress-strain curves, the obtained strength and modulus of elasticity of the GFRP coupons, and a comparison of compressive and tensile characteristics of the GFRP bars.

Failure Modes

In this study, three main modes of failure were observed including crushing of GFRP bar only in the free length, crushing of GFRP bars only inside the capping, and crushing both inside the capping and in the free length. It should be noted that no buckling of the GFRP bars were observed for the tested specimens. Fig. 6 presents some specimens that were crushed in the free length [Fig. 6(a)] as well as some GFRP coupons that reached the peak load without any visible sign in the free length [Fig. 6(b)]. The crushing of GFRP bars happened to be at the middle or close to the ends of

the bars, and some the failure line was either horizontal or diagonal, as shown in Fig. 6(a). It should be mentioned that crushing in the free length of the specimens observed in 56% of the tested specimens. For the rest of the specimens, there were no visible sign of the failure in the free length, as presented in Fig. 6(b). However, the stress-strain graphs for both types of failure was similar to each other, and no difference in compressive strength or modulus of elasticity of these two groups were observed. For further investigations, the specimens were cut in half longitudinally after testing. Three different types of observed failures are presented in Fig. 7. The observations showed that for the specimens which experienced non-visible failure, the GFRP bars were crushed inside the capping area, while the capping agent and steel cap did not fail. Therefore, the modes of failure for the proposed test method can be categorized as crushing of GFRP bar only in the free length, crushing of the GFRP bar only inside the capping, and crushing of the GFRP bar both inside the capping and in the free length.

Fig. 8 presents the failed compressive coupons from group G4 to G7. In terms of modes of failure, it should be highlighted that crushing of the GFRP bars inside the capping or in the free length were randomly distributed for the tested specimens, as shown in Fig. 8. In terms of the duration of the test, depends on the mode of failure, the test duration varied. For most of the specimens whose failure was only in the free length, failure happened with a sudden drop in the load carrying capacity and the tests were concluded [Fig. 7(a)]. However, for specimens experiencing the GFRP bar failure only inside the capping or both inside the capping and in the free length, the tests last longer [Fig. 7(b) and 7(c)]. For the latter case, it could be implied that the failure was progressive, started locally from some fibers, and propagated to reach the final crushing of the whole bar which was corresponding to dropping in the load capacity. The tests were concluded in about an average of 4.6, 14.4, and 11.8 minutes for specimens which experienced

failure only in the free length, both in free length and inside capping, and for those whose failure occurred only inside capping, respectively. However, by measuring the strain rate of the specimens between two strains of 0.001 to 0.003 mm/mm, the strain rate of 0.0024 mm/mm/min was recoded for all specimens regardless of failure type.

Overall, the tests predicted consistent results for the modulus of elasticity and compressive strength of the GFRP specimens regardless of the location of the failure in GFRP bars or the duration of the tests. However, the ultimate crushing strain cannot be determined based on the results of the strain gauges or the reading of the axial displacement directly. Since the progressive nature of failure for the specimens which experienced failure inside the capping lead to successive gain and drop in the strain, the ultimate strain might be indistinguishable. Therefore, to calculate the crushing strain, reporting a nominal value is suggested when the proposed test method is used. The latter can be done by dividing the compressive strength by modulus of elasticity according to the Hooke's law; since the stress-strain behavior of the specimens shows a linearity as presented in the following section.

Stress-Strain Behavior

The stress-stain curves for all seven groups of tested compressive coupons (each including five specimens) is presented in Fig. 9. The stress-strain curve for each compressive coupon was derived by averaging the strain values recorded from two strain gauges at the opposite side at the middle of the GFRP coupon like the procedure that was suggested by ASTM D7205 [17] for testing GFRP bars in tension. For group G1, it was seen that the stress-strain curves were continued up to the crushing point and the load suddenly dropped after the failure. For all specimens in this group, the GFRP bar failure happened only in the free length of the specimens. It was observed that the stress-strain curves for different specimens in the same group were linear and tightly close to each other,

which showed the consistency of the test results. Moreover, the average stress-strain line was very close to the curves for every single specimen. Therefore, the average gave good approximation of the compressive stress-strain behavior of the GFRP bars in compression. The average stress-strain lines were obtained using the average of strength and modulus of elasticity for every single specimen in a group, shown as the dashed line in Fig. 9. The average compressive modulus of elasticity and compressive strength for all groups as well as their standard deviation and coefficient of variation is presented in Table 3. The results showed consistency of the proposed test method in the determination of the strength and modulus of elasticity due to obtaining a small coefficient of variations for strength and modulus of elasticity. The average stress-strain curves for all groups are presented in Fig. 9(h).

For group G2, some of the strain gauges were broken after a certain load and the strain recording was not available after that point, as shown in Fig. 9(b). The problem that caused the separation of the strain gauges from the GFRP bars was improved by enhancing the surface preparation of the strain gauges for the other groups as explained in the preparation section of this paper.

For group G4, it was observed that the slope of the stress-strain curves deviated as the load increased, as shown in Fig. 9(d). For all group G4, the progressive failure happened only inside the capping since the GFRP crushing happened only in the capping, as shown in Fig. 8. Therefore, the drop and gain of the strain and the stress in the stress-strain curves were occurred as presented in Fig. 9(d). However, for the specimens in group G5, which had the same diameter and produced by the same manufacturer as group G4, all the specimens experienced linear stress-strain curves without any drop and gain in the strain and the stress. It was observed that the mode of failure for specimens in group G5 was either crushing of the bar in the free length or both inside capping and

in the free length. Therefore, there should be a meaningful relation between the failure mode and the stress-strain curves. It was observed that for the specimens which experienced crushing only in the free length, there was no drop and gain in the strain and the stress up to failure. In other words, the progressive failure inside the capping could be recognized from the shape of the stress-strain curves.

Since the specimen in group G5 had higher modulus of elasticity, it might be implied that for GFRP bars with higher modulus of elasticity, the failure mode is dictated to be in the free length. However, observation of the results of group G6 and G7 which were produced by the same manufacturer and had the same diameter showed that higher modulus does not necessarily control the mode of failure. For example, specimens in group G7 has higher modulus of elasticity than the specimens in group G6, but the drop and gain in the strain and the stress in the stress-strain curves were mainly observed in group G7, as shown in Fig. 9(f) and 9(g). The latter is in contrast with the results of the comparison made between group G4 and G5 as discussed earlier. Also, it was observed that for group G6 and G7, the failure modes were random, as shown in Fig 8.

Determination of Compressive Characteristics

It was observed that the proposed test method leads to three different modes of failure which causes a drop or gain in the stress and the strain values for some specimens based on the mode of failure as discussed earlier. However, it should be mentioned that the drop and gain of the stress and the strain in the stress-strain curves started after a certain strain that was greater than 0.005 mm/mm for all specimens, as shown in Fig. 9. Thus, for the calculation of compressive modulus of elasticity of GFRP bars, the portion of the stress-strain curves that lies between the strain values of 0.001 and 0.003 mm/mm was used, which is compatible with ASTM D7205 [17] suggestion for derivation of the tensile modulus of elasticity for the GFRP bars, as shown in Fig. 10. Therefore,

the mode of failure cannot have any effect on the calculation of the compressive modulus of elasticity based on the results of the experimental tests. In this paper, the compressive modulus of elasticity was determined as the slope of the linear trendline that passes through the average of two strain gauges for each specimen. Then, the average, standard deviation, and coefficient of variation of five identical specimens in each group were obtained and presented in Table 3. The test results revealed that the coefficient of variation for determination of compressive modulus of elasticity was 2.54% which showed that the proposed test method measured the modulus of elasticity of the specimens very consistently.

The average and standard deviation for compressive strength of all groups is presented in Table 3. As mentioned earlier, there were three different modes of failure including crushing of GFRP only in the free length, only inside the capping, or both inside the capping and in the free length. The consequence of the crushing of the GFRP bar inside the capping was progressive failure and observing a drop and gain of the stress and strain in the stress-strain curves. The latter did not allow a unique crushing strain to be recognized by the proposed test method for all the specimens. Therefore, the ultimate crushing strains were derived by dividing the compressive strength by the compressive modulus of elasticity, as presented in Table 3. However, there was no difference between the specimens with different modes of failure in terms of determining their compressive strength and modulus of elasticity. The average coefficient of variation for determination of compressive strength for all tested specimens was 7.07% which shows an acceptable range of results and consistent values for the compressive strength of GFRP bars.

Comparison of Compressive and Tensile Properties

The average compressive modulus of elasticity and strength of each group of GFRP bars as well as the reported tensile properties of GFRP bars are presented in Table 3. It was seen that the

modulus of elasticity in compression and tension are quite close, and the strength is lower in compression. The compressive to tensile modulus of elasticity and strength ratios for the tested groups is presented in Fig. 11 and Table 3. It was observed that the modulus of elasticity in compression, in average, was between 97% to 120% of the modulus of elasticity in tension. Moreover, the average compressive strength was between 55% to 99% of the tensile strength. Overall, the average of the compressive to tensile modulus of elasticity and strength ratios were 0.81 and 1.04, respectively. The latter shows that the modulus of elasticity of GFRP bars in compression can be considered the same as in tension. However, for determining the compressive strength, the compressive test is necessary due to the wide variety of compressive to tensile strength ratios. In other words, the test of GFRP bars in tensile is not sufficient to estimate the compressive strength of the GFRP bars.

Design Recommendation

The proposed test method and the experimental program presented in this paper showed that the modulus of elasticity of GFRP bars in compression can be considered the same as the one in tension. In addition, the compressive to tensile strength ratio of the GFRP bars, tested in this study, was between 55% to 99%. The latter means, the GFRP bars was able to support a compressive strain ranging from 0.0103 to 0.0193 mm/mm. The range was way beyond the design strain of 0.003 and 0.0035 mm/mm which were specified by ACI 318 [20] and CSA A23.3 [21], respectively. This means the contribution of GFRP bar in concrete members, can be calculated by multiplying the modulus of elasticity by the calculated strain of GFRP bar when the ultimate compressive fiber in concrete reaches to the specified design strain. It should be mentioned that the strain in GFRP bar can be calculated based on the linear stain distribution in the cross section and based on the loading condition of the considered system.

CONCLUSIONS

This paper was dedicated to determination of the compressive strength, compressive modulus of elasticity, the crushing strain, and compressive stress-strain curve of GFRP bars by proposing a new test method. A total of 35 GFRP bar compressive coupons were built and tested using the proposed test method which covered three different bar diameters, provided by three different manufacturers. The following conclusions can be drawn:

- The proposed test method was successfully implemented to obtain the compressive modulus of elasticity, compressive strength, ultimate crushing strain, and compressive stress-strain curve of the GFRP bars.
- The results of the experimental study showed no buckling of GFRP bars as a mode of failure. Three different modes of failure were observed: i) crushing of GFRP bars only in the free length; ii) crushing of the GFRP bars only inside the capping; iii) crushing of GFRP bars both inside the capping and in the free length. It should be highlighted that 56% of specimens experienced crushing of the GFRP bar in the free length while for the rest of the specimens there was no sign of crushing in the free length.
- It was observed that the compressive modulus of elasticity and strength of GFRP bars, which was assessed using the proposed test method, were not affected by the difference in the modes of failure. However, the crushing strain cannot be evaluated directly from the test for the cases that experience GFRP crushing inside capping.
- It was observed that considering a linear behavior for the compressive stress-strain curves of GFRP bars was a good assumption. Therefore, the crushing strain was reported by dividing the compressive strength by the compressive modulus of elasticity.

- The average coefficient of variation of compressive strength and modulus of elasticity for all tested groups were 7.07% and 2.54%, respectively, which shows that very consistent results can be obtained using the proposed method.
- The average of compressive to tensile modulus of elasticity and strength ratios varied from 0.97 to 1.20 and from 0.55 to 0.99, respectively, for different groups of the tested specimens. In average, the compressive to tensile strength and the modulus of elasticity ratios for all specimens were 1.04 and 0.81, respectively. The latter shows that the modulus of elasticity in compression and tension could be considered the same for GFRP bars. However, because of the wide range of variation in the ratio of the compressive to tensile strength, the tensile test of GFRP bars is not sufficient to estimate the compression strength. Therefore, performing a compression test is necessary for determination of the compressive strength of GFRP bars.

ACKNOWLEDGEMENTS

Authors would like to thank Jordan Maerz, Jesse Keane, and Brian Kennedy for their assistance in the lab. The authors would also like to acknowledge and thank NSERC and Dalhousie University for their financial support. Aslan FRP, V-ROD Canada, and TUF-BAR companies are thanked for providing GFRP bars.

REFERENCES

[1] ACI 440.1R, "Guide for the Design and Construction of Structural Concrete Reinforced Fiber-Reinforced Polymer (FRP) Bars," American Concrete Institute, Farmington Hills, MI, 2015.

[2] CAN/CSA S806, "Design and Construction of Building Structures with Fibre-Reinforced Polymers," Canadian Standards Association, Mississauga, Ontario, 2012.

[3] Guérin, M., Mohamed, H. M., Benmokrane, B., Nanni, A., and Shield, C. K.,"Eccentric Behavior of Full-Scale Reinforced Concrete Columns with Glass Fiber-Reinforced Polymer Bars and Ties," ACI Structural Journal, Vol. 115, No. 2, 2018, pp. 489-499, https://doi.org/10.14359/51701107 .

[4] Fillmore, B. and Sadeghian, P., "Contribution of Longitudinal Glass Fiber-Reinforced Polymer Bars in Concrete Cylinders under Axial Compression," Canadian Journal of Civil Engineers, Vol. 45, 2018, pp. 458-468, https://doi.org/10.1139/cjce-2017-0481 .

[5] Khorramian, K. and Sadeghian, P., "Experimental and Analytical Behavior of Short Concrete Columns Reinforced with GFRP Bars under Eccentric Loading," Engineering Structures, Vol. 151, 2017, pp. 761–773, https://doi.org/10.1016/j.engstruct.2017.08.064 .

[6] Hales, T. A., Pantelides, C. P., and Reaveley, L. D., "Experimental Evaluation of Slender High-Strength Concrete Columns with GFRP and Hybrid Reinforcement," Journal of Composites for Construction, Vol. 20, No. 6, 2016, pp. 04016050, https://doi.org/10.1061/(asce)cc.1943-5614.0000709 .

[7] Mohamed, H. M., Afifi, M. Z., and Benmokrane, B., "Performance Evaluation of Concrete Columns Reinforced Longitudinally with FRP Bars and Confined with FRP Hoops and Spirals under Axial Load," Journal of Bridge Engineering, Vol. 19, No. 7, 2014, pp. 04014020, https://doi.org/10.1061/(asce)be.1943-5592.0000590 .

[8] Tobbi, H., Farghaly, A. S., and Benmokrane, B., "Concrete Columns Reinforced Longitudinally and Transversally with Glass Fiber-Reinforced Polymer Bars," ACI Structural Journal, Vol. 109, No. 4, 2012, pp. 551-558, https://doi.org/10.14359/51683874.

[9] CAN/CSA S6 , "Canadian Highway Bridge Design Code," Canadian Standards Association, Mississauga, Ontario, 2014.

[10] Sheikh, S. and Kharal, Z., "GFRP-Reinforced Concrete Columns Subjected to Seismic Loads," ACI Special Publication, SP 326, 2018, Vol 326, pp. 56-1:10.

[11] Tavassoli, A., Liu, J., and Sheikh, S., "Glass Fiber-Reinforced Polymer-Reinforced Circular Columns under Simulated Seismic Loads," ACI Structural Journal, Vol. 112, No.1, 2015, pp. 103-114, https://doi.org/10.14359/51687227 .

[12] Kobayashi, K. and Fujisaki, T., "Compressive Behaviour of FRP Reinforcement in Non Prestressed Concrete Members," Non Metallic (FRP) Reinforcement for Concrete Structures, Proceedings of the Second International RILEM Symposium (FRPRCS-2), London, UK, 1995, pp. 267-274.

[13] Deitz, D. H., Harik, I. E. and Gesund, H., "Physical Properties of Glass Fiber Reinforced Polymer Rebars in Compression," Journal of Composites for Construction, ASCE, Vol. 7, No. 4, 2003, pp. 363-366, https://doi.org/10.1061/(asce)1090-0268(2003)7:4(363) .

[14] Khan, Q. S., Sheikh, M. N., and Hadi, M. N. S., "Tension and Compression Testing of Fibre Reinforced Polymer (FRP) Bars," Joint Conference of the 12th International Symposium on Fiber Reinforced Polymers for Reinforced Concrete Structures (FRPRCS-12) & the 5th Asia Pacific Conference on Fiber Reinforced Polymers in Structures (APFIS-2015), Nanjing, China, 2015, pp.1-6.

[15] ASTM D695, “Standard Test Method for Compressive Properties of Rigid Plastics,” Annual Book of ASTM Standards, ASTM International, West Conshohocken, PA, 2010, www.astm.org.

[16] Khorramian, K. and Sadeghian, P., "New Testing Method of GFRP Bars in Compression," Canadian Society for Civil Engineering, Fredericton, NB, Canada, 2018, pp. MA7:1-9.

[17] ASTM D7205 / D7205M, “Standard Test Method for Tensile Properties of Fiber Reinforced Polymer Matrix Composite Bars,” Annual Book of ASTM Standards, ASTM International, West Conshohocken, PA, 2016, www.astm.org.

[18] ASTM D6641/D6641M, “Standard Test Method for Compressive Properties of Polymer Matrix Composite Materials Using a Combined Loading Compression (CLC) Test Fixture,” Annual Book of ASTM Standards, ASTM International, West Conshohocken, PA, 2016, www.astm.org.

[19] ASTM C39/C39M, “Standard Test Method for Compressive Strength of Cylindrical Concrete Specimens,” Annual Book of ASTM Standards, ASTM International, West Conshohocken, PA, 2018, www.astm.org.

[20] ACI 318, "Building Code Requirements for Structural Concrete," American Concrete Institute, Farmington Hills, MI, 2014.

[21] CAN/CSA A23.3, "Design of Concrete Structures," Canadian Standard Association, Mississauga, Ontario, 2014.

Table 1 Previously used test methods.

No.	Reference	Free length (mm)	Bar diameters (mm)	Free length to diameter ratio	Gripping type	Grip length (mm)	Grip section (mm)	Loading rate (mm/min)
1	Kobayashi and Fujisaki [12]	5	6, 8, 10,13	0.83, 0.63, 0.50, 0.38	Carbon anchorage cones embedded in concrete prisms	197.5	Rectangular (125× 180 mm)	NA
2	Dietz et al. [13]	50 - 380	15	3.33 - 25.33	Threaded steel rod with a hole at the middle	135	Circular (50 mm)	NA
3	Khan et al. [14]	80, 60	16, 15	5.03, 4.00	No gripping (grips were replaced with two high strength steel plates.)	-	-	1 -1.3
4	Tavassoli et al. [11]	50, 60, 275	25	2.00, 2.40, 11.00	Threaded steel rod with a hole at the middle	NA	Circular	NA
5	Khorramian and Sadeghian [16]	26, 32, 38	13, 16, 19	2.00	Steel pipe welded at one end and filled with quick set high strength adhesive	13, 16, 19	Circular (50 mm)	0.5

Note: NA = not available.

Table 2 Experimental test matrix.

No.	Group	GFRP bar size	Nominal diameter (mm)	Nominal Area (mm^2)	E_t (GPa)	f_t (MPa)	Specimen IDs	Manufacturer
1	G1[a]	#4	13.0	126.7	46	758	G1-1, G1-2, G1-3, G1-4, G1-5	A
2	G2[b]	#5	16.0	197.9	42.5	940	G2-1, G2-2, G2-3, G2-4, G2-5	B
3	G3[c]	#6	19.0	285.0	46	690	G3-1, G3-2, G3-3, G3-4, G3-5	A
4	G4	#4	12.5	129.0	45.6	845.4	G4-1, G4-2, G4-3, G4-4, G4-5	C
5	G5	#4	13.9	129.0	61.1	1175	G5-1, G5-2, G5-3, G5-4, G5-5	C
6	G6	#6	19.2	284.0	51	884.3	G6-1, G6-2, G6-3, G6-4, G6-5	C
7	G7	#6	20.7	284.0	62.7	1150	G7-1, G7-2, G7-3, G7-4, G7-5	C

Note: E_t = tensile modulus of elasticity of GFRP bars; f_t = tensile strength of GFRP bars.
[a] Adopted from Fillmore and Sadeghian [4].
[b] Adopted from Khorramian and Sadeghian [5].
[c] Adopted from Khorramian and Sadeghian [16].

Table 3 Comparison of compression and tensile properties of tested GFRP coupons.

Group	f_t^* (MPa)	E_t^* (GPa)	$f_{c,ave}$ (MPa)	$E_{c,ave}$ (GPa)	σ_{fc} (MPa)	σ_{Ec} (GPa)	ε_c (mm/mm)	CoV_{fc} (%)	CoV_{Ec} (%)	R1	R2
G1	758	46	559	45.78	36	2.15	0.0122	6.36	0.05	0.74	1.00
G2	940	42.5	795	41.16	69	1.16	0.0193	8.74	2.81	0.85	0.97
G3	690	46	684	48.89	33	0.89	0.0140	4.83	1.83	0.99	1.06
G4	845.4	45.6	790	54.51	23	3.38	0.0145	2.91	6.19	0.93	1.20
G5	1175	61.1	652	63.46	38	1.98	0.0103	5.84	3.12	0.55	1.04
G6	884.3	51	683	51.19	75	0.77	0.0134	11.00	1.51	0.77	1.00
G7	1150	62.7	940	63.44	92	1.44	0.0148	9.82	2.27	0.82	1.01
Average								7.07	2.54	0.81	1.04

Note: E_t = tensile modulus of elasticity of GFRP bars; f_t = tensile strength of GFRP bars; E_c = average compressive modulus of elasticity of GFRP bars; f_c = average compressive strength of GFRP bars; ε_c = ultimate compressive strain of GFRP bars; σ_{Ec} = standard deviation of compressive modulus of elasticity of GFRP bars; σ_{fc} = standard deviation of compressive strength of GFRP bars; CoV_{Ec} = coefficient of variation of compressive modulus of elasticity of GFRP bars; CoV_{fc} = coefficient of variation of compressive strength of GFRP bars; R1 = the ratio of average compressive to tensile strength of GFRP bars; R2 = the ratio of average compressive to tensile modulus of elasticity of GFRP bars.
*The tensile properties used in this table were reported by the manufacturers.

List of Tables

List of Figures:

FIG. 1 Compressive GFRP coupon components and geometry.

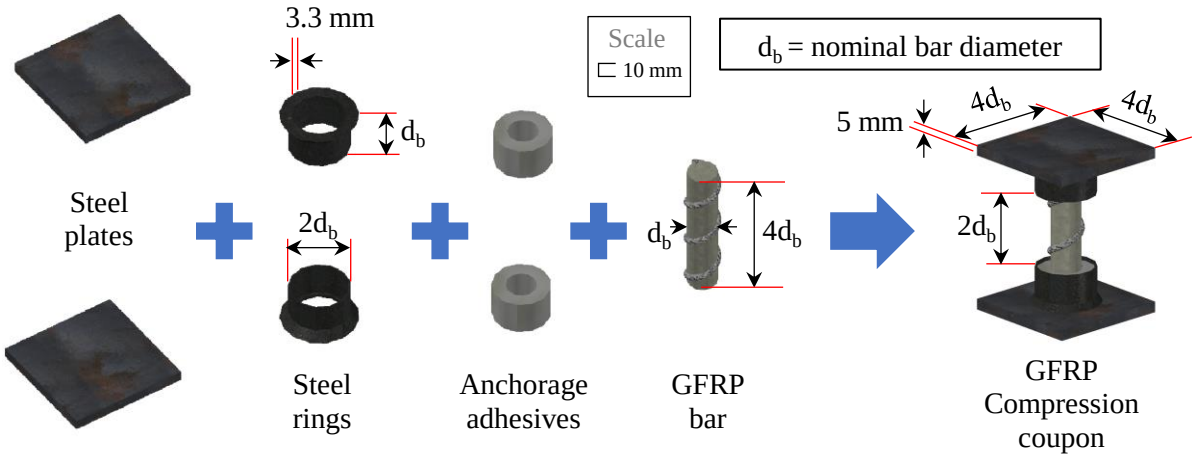

FIG. 2 Fabrication process and a prepared GFRP compressive coupon.

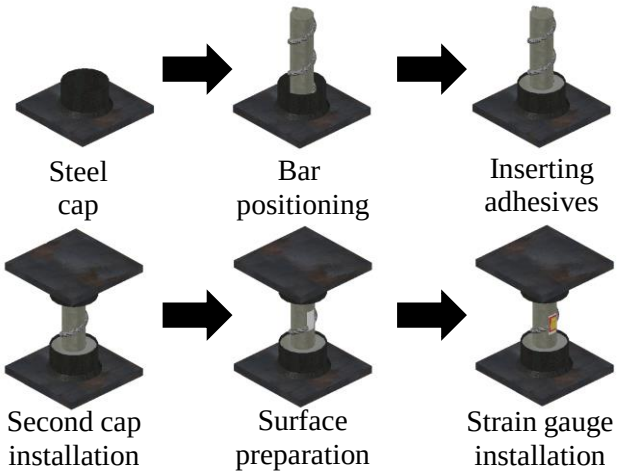

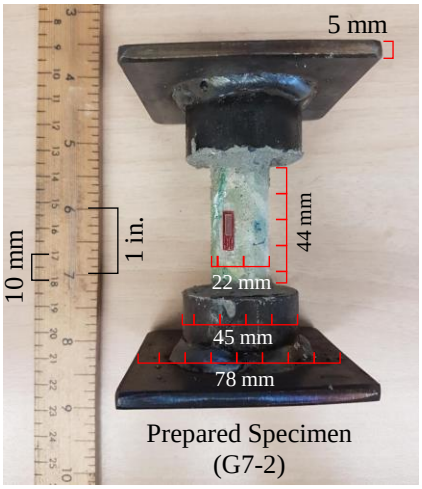

FIG. 3 Prepared specimens for group G6.

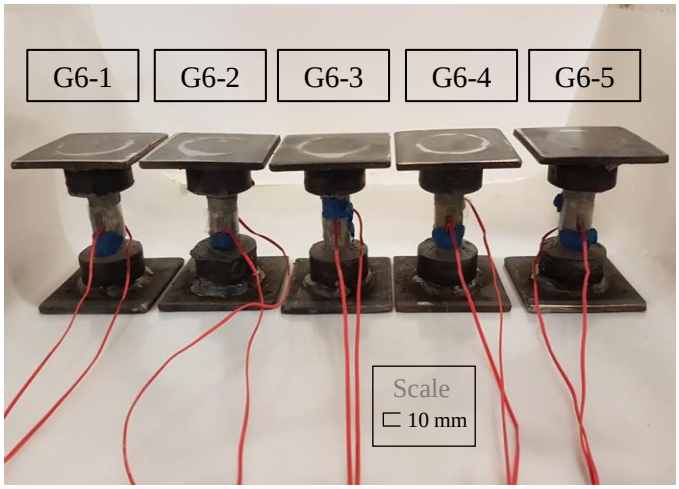

FIG. 4 Schematic test set-up and instrumentation.

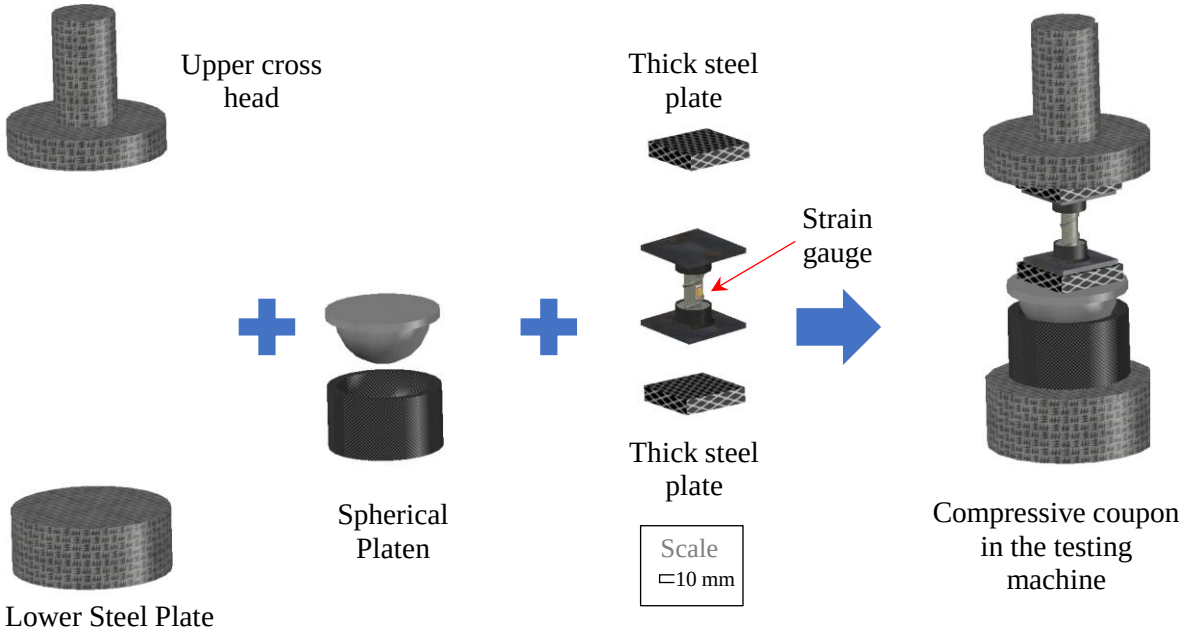

FIG. 5 G6-1 specimen in the testing machine.

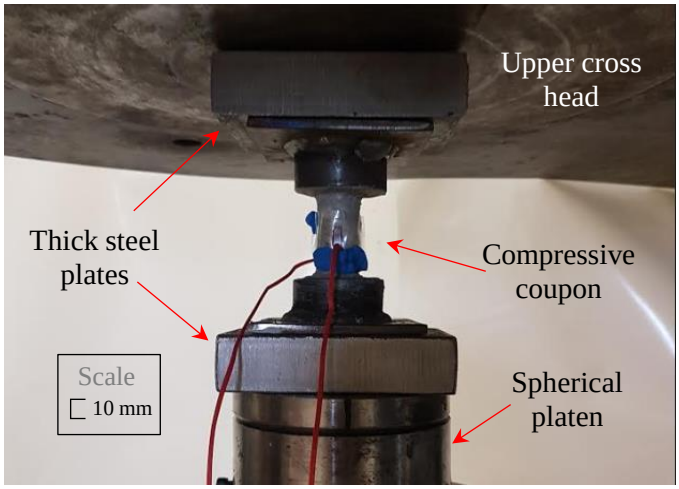

FIG. 6 Modes of failure: (a) crushing of GFRP bar, (b) failure inside capping.

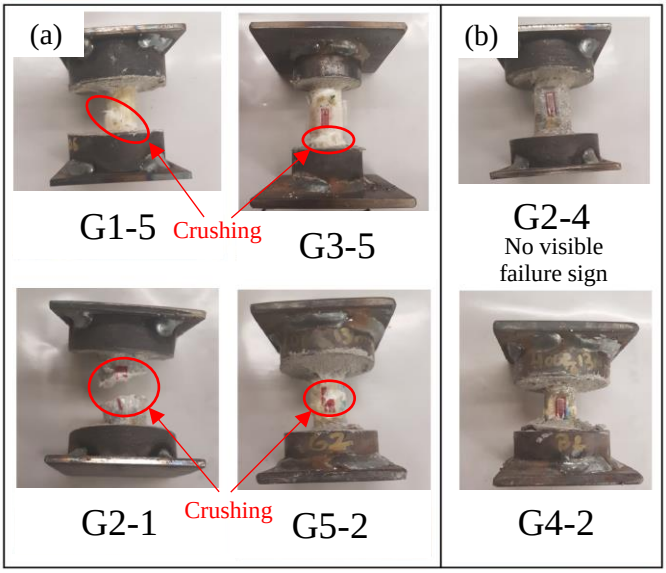

FIG. 7 Modes of failure: (a) crushing of GFRP bar in the free length, (b) crushing of GFRP bar inside the capping, (c) crushing of the GFRP bar both inside capping and in the free length.

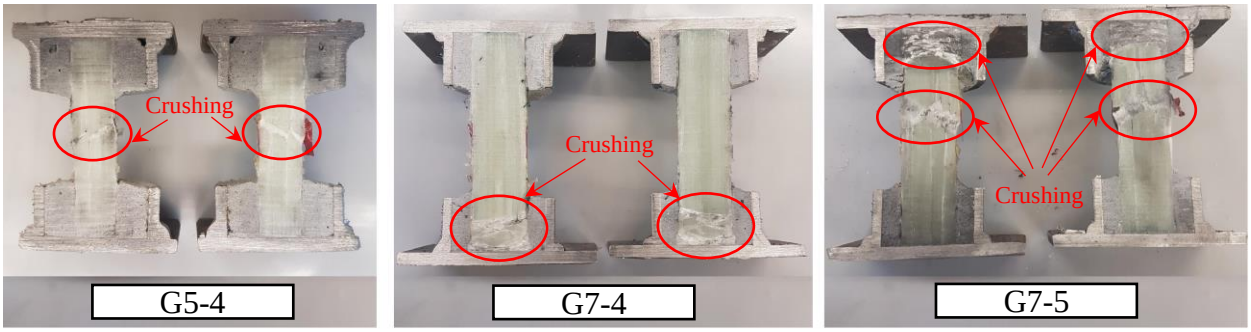

(a) (b) (c)

FIG. 8 Failed specimens: (a) G4 and G5 groups, (b) G6 and G7 groups.

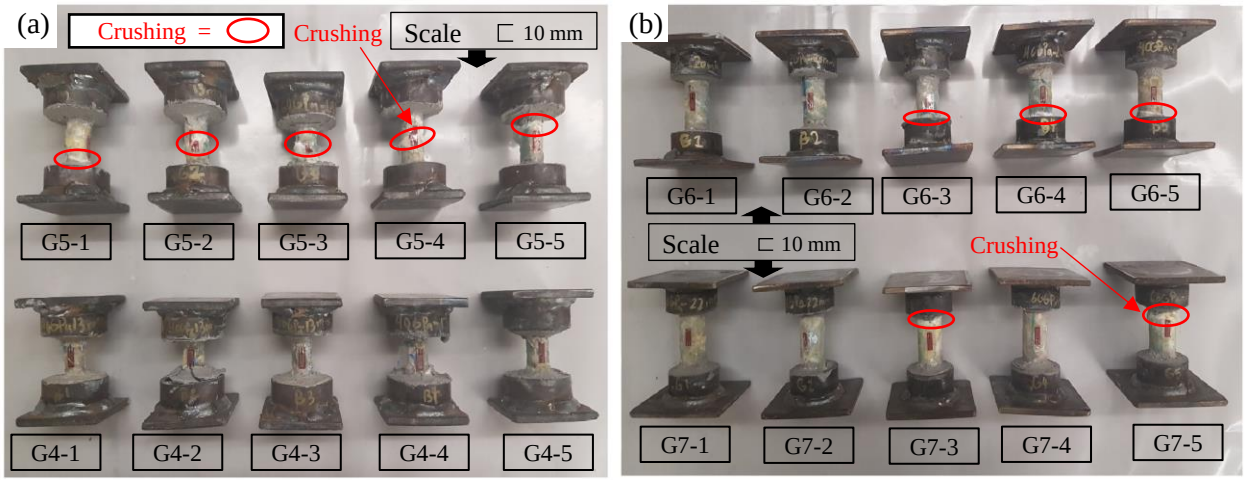

FIG. 9 Stress-strain curves: (a) G1, (b) G2, (c) G3, (d) G4, (e) G5, (f) G6, (g) G7, (h) Summary.

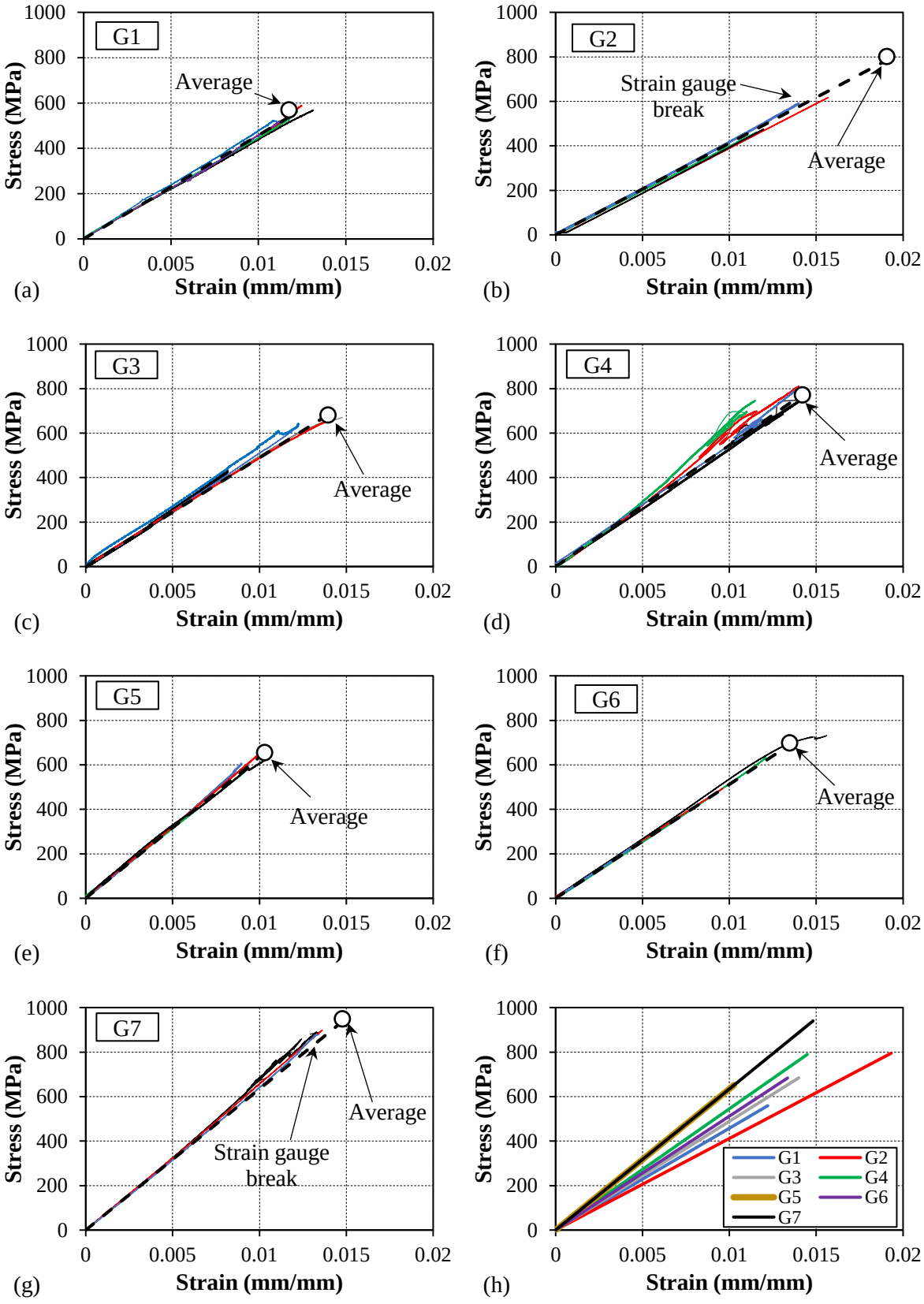

FIG. 10 Determination of modulus of elasticity.

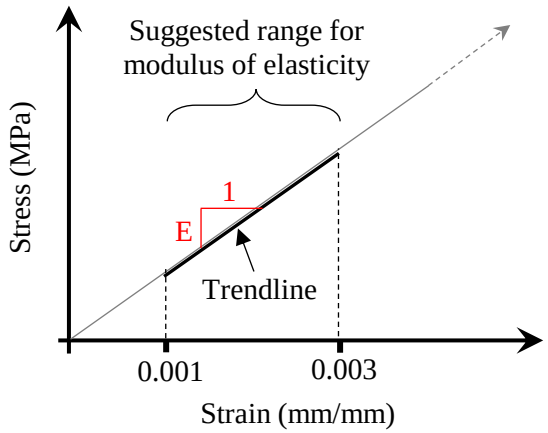

FIG. 11 Ratio of compressive to tensile modulus of elasticity and strength.